Food Research 6 (3) : 12 - 20 (June 2022)
Journal homepage: https://www.myfoodresearch.com

FOOD RESEARCH

FULL PAPER

Moisture content and application rates of inert dust: effects on dust and wheat physical properties

[1,*]Yao, K.D., [1]Subramanyam, B. and [2]Maghirang, R.G.

[1]*Department of Grain Science and Industry, Kansas State University, Manhattan, KS 66506, United States of America*
[2]*Department of Biological and Agricultural Engineering, Kansas State University, Manhattan, KS 66506, United States of America*

Article history:
Received: 18 May 2021
Received in revised form: 2 June 2021
Accepted: 23 August 2021
Available Online: 5 May 2022

Keywords:
Particle size,
Particle shape,
Flow properties,
Post-harvest technology,
Wheat,
Agriculture

DOI:
https://doi.org/10.26656/fr.2017.6(3).280

Abstract

Grain protectants such as inert dust help prevent quality deterioration during post-harvest storage. Understanding the physical characteristics of inert dust and inert dust treated wheat kernels could help develop solutions to flow problems of stored grain. This research investigated the effects of the moisture content of a synthetic amorphous zeolite and the rates of application on some physical properties of the amorphous zeolite and wheat kernels. Three levels of moisture (2.0%, 6.0%, and 10.0%) of the zeolite were applied at three rates (0.5 g/kg, 1.0 g/kg, and 2.0 g/kg) on 100 g wheat samples (10% m.c, wet basis) in triplicates. Image analysis, laser diffraction, Thermogravimetric analysis (TGA), Scanning Electron Microscopy (SEM), gas pycnometry, and the Single-Kernel Characterization System (SKCS) were used to characterize the physical properties. The particle size of the amorphous dust increased with increasing moisture content. Conversely, shape parameters (circularity, aspect ratio, convexity, and solidity) generally decreased with increasing dust moisture contents. When wheat was mixed with the amorphous dust at increasing rates and moisture levels, the bulk density of wheat decreased, while the tapped density and the angle of repose increased, resulting in higher Hausner ratios and Carr Index values. Treating wheat with the amorphous dust at the highest moisture (35%) and application rate (2.0 g/kg) caused the treated wheat to transition from an acceptable flowability to a poor flowability along with a decrease in wheat kernel hardness. Our data suggest, however, that a range of moisture content (2-6%) and an application rate (0.5 g/kg) mitigate the adverse effects on wheat flowability. This study also highlights the importance of drying any amorphous dust or allowing dust to equilibrate to the experiment temperature before conducting tests on physical properties.

1. Introduction

Inert dust, like most powders, is not solely discrete solid particles, but rather a mixture of solid, liquid (surface moisture content), and gas (entrapped air). Wheat kernels treated with inert dust form a granular system, which can transition between any of three distinct states: static, quasi-static, or dynamic (Lumay *et al.*, 2012). A major concern, when applying any amorphous dust onto grain for quality preservation, is the change in the flow properties of the treated grain. A good flowability of wheat treated with inert dust and stored in bins or silos is the ability of wheat kernels to easily exit the bin or silo by exhibiting low particle-to-particle friction and low particle to bin or silo inner wall surface friction. Ideally, wheat kernels with low surface friction, a low angle of repose, a low angle of internal friction, a low angle of wall friction, and low compressibility are needed for optimal flow properties and minimal energy requirement during mechanical handling. When amorphous inert dust is mixed with coarser materials such as grain kernels, the overall flow properties are influenced by the amount of dust in the mixture, the particle shape and surface roughness of the dust particles, and moisture content of the dust, and moisture content of grain kernels. The handling history, the state of compaction, the storage duration, and the process involved are important factors to consider. A vast array of literature exists that stresses the relationship between flowability and grain physical properties such as particle size, particle shape, moisture, and environmental parameters such as temperature, and relative humidity

*Corresponding author.
Email: *kdyao@ksu.edu*

eISSN: 2550-2166
Published by Rynnye Lyan Resources

(Fitzpatrick *et al.*, 2004; Iqbal and Fitzpatrick, 2006; Freeman and Cooke, 2006; Freeman, 2007; Ganesan, 2008; Emery *et al.*, 2009). Increasing grain moisture content generally causes a decrease in grain bulk density (Altuntaş and Yıldız, 2007). However, the moisture content of the inert dust applied onto grain can also influence grain moisture content, and hence grain bulk density. Grain bulk density is a key indicator of wheat quality and is used to grade and assess the commercial value of any class of wheat. For instance, the minimum bulk density to meet the requirements for U.S. grade No.1, is 60 pounds per bushel, except for Hard Red Spring wheat or White Club wheat (58 pounds per bushel). The extent of the decrease in bulk density may vary with the type and amount of dust, the particle size, and the moisture content of the dust. More importantly, a lower bulk density may not necessarily translate into poor flow performance. In other words, the magnitude of change in bulk density is not a good indicator of the magnitude of change in flow properties. The changes in shape and size, as well as the surface roughness of particles of porous powders used as grain protectants, are likely to alter the flow and abrasive properties of wheat kernels. However, it is unclear whether moisture content will affect the particle size and shape of porous inert dust. Particle size analysis is often conducted to determine and evaluate the modifications in particle size. Particle size analysis alone does not always discriminate between particles with different shapes. Thus, particle shape analysis is quite often carried out in addition to particle size analysis. Particle shape factors help shed light on subtle differences that may exist between particles of identical size, thus contributing to a better understanding of flow properties. Particle shape was shown to have a significantly higher impact on grain flowability (Fu *et al.*, 2012). Several methods exist to quantify particle size and shape. Laser diffraction uses the Mie theory of light scattering to calculate the particle size distribution, assuming a volume equivalent sphere model. Mie theory requires knowledge of the optical properties of both the dispersant and the sample being measured. A simplified approach is to use the Fraunhofer approximation, which does not require the optical properties of the sample. Mie theory is detailed elsewhere in the literature (Fu and Sun, 2001; Eshel *et al.*, 2004; Andrews *et al.*, 2010; Niskanen *et al.*, 2019). Automated image analysis is a counting technique that gives a number weighted distribution where each particle is given equal weighting irrespective of its size. Eggers *et al.* (2008) have extensively covered the measurement of particle size and shape using image analysis. Understanding the relationship between the moisture content and particle size and particle shape can help better predict the flowability of the treated grain. The objectives of this study were: to characterize the physical properties of a synthetic amorphous zeolite; to determine the influence of inert dust moisture content on inert dust particle size, shape, and surface roughness; and to determine the influence of inert dust moisture content and application rates on some physical properties of wheat kernels.

2. Materials and methods

2.1 Physical characterization of a synthetic amorphous zeolite

The physical characterization of the synthetic amorphous zeolite was performed at an as-is moisture content of 35.5% (dry basis). The moisture content of zeolite was determined by Thermogravimetric Analysis (TGA) method. The amorphousness of synthetic zeolite was confirmed using X-ray diffraction (Empyrean, Pananalytical). Particle size distribution was determined by laser diffraction (Mastersizer 3000, Malvern). The average particle size and shape of synthetic zeolite were determined using image analysis (Morphologi G3, Malvern). The average pore size and pore distribution of zeolite were determined using nitrogen physisorption. The specific surface area of individual particles was determined using BET tests. Surface images to characterize the surface texture were obtained by Scanning Electron Microscopy (SEM).

2.2 Moisture effects on physical properties of an amorphous silica dust

2.2.1 Sampling

A fresh batch of a synthetic amorphous zeolite, Odor -Z-Way®, available in the market as an odour absorbent, was purchased from a local manufacturer (Odor-Z-Way®, Phillipsburg, KS, USA). Measurements samples were obtained by passing gross samples through a chute splitter device. A total of 27 measurement samples were obtained and 9 samples were systematically selected and randomly assigned, in triplicates, to each of three moisture levels (2.0, 6.0, and 10.0%).

2.2.2 Equilibration in a controlled humidity chamber

The initial moisture content determined by thermogravimetric analysis (TGA) (Pyris 1 TGA, Perkin Elmer) was about 35% (dry basis). Zeolite samples were then dried overnight at 25°C to remove excess moisture. Moisture content was re-determined by TGA and was about 1.29% (d.b.). Samples of zeolite were then allowed to equilibrate to 2±0.05%, 6±0.02%, and 10±0.01% moisture contents in controlled humidity chambers at 25° C under a specific relative humidity (Table 1). Each equilibrium relative humidity was based on the adsorption isotherm of the synthetic zeolite at 25°C.

Equilibrium was achieved when the relative change in sample weight did not exceed 1%. The samples were immediately analyzed once equilibrium was reached to minimize exposure to laboratory ambient conditions.

Table 1. Equilibration parameters of zeolite powder and wheat kernels in a controlled humidity chamber at 25°C

	Relative Humidity (%)	Equilibrium moisture contents (%)	Time to reach equilibration (h)
Zeolite	27.7	2.01	14.55
	63.6	6.03	17.0
	75.2	10.02	19.4
Wheat	28.3	10.0	10.1

2.2.3 True density analysis

The true density of a particle is the mass of a particle divided by its true volume, excluding open and closed pores. True density was measured using a gas displacement pycnometer (Helium AccuPyc 1330, Micromeritics, Norcross, Georgia, USA). Helium gas was used to fill a chamber containing the sample and small voids (pores) within the sample to determine the volume occupied by the particles. The principle is that Helium gas, under precisely known pressure, occupies a fixed volume. The change in volume of Helium in a constant volume chamber allows the determination of solid volume. The ratio of sample mass to its true (solid) volume yields the true density. The data was collected through an RS-232 cable connected to a computer.

$$\text{True density} = \frac{\text{Weight (g)}}{\text{True volume (cm}^3\text{)}} \quad (1)$$

2.2.4 Particle size and shape analysis

Data from particle and shape analysis fully characterize both spherical and irregularly-shaped particles. Particle size distribution, surface weighted mean (Sauter mean), and volume-weighted mean (De Brouckere mean) were determined by laser diffraction (Mastersizer 3000, Malvern). Shape factors such as particle diameter (CE diameter), particle form (aspect ratio, elongation), particle outline (convexity, solidity), and a universal shape parameter (circularity) were determined by automated image analysis (Morphologi G3, Malvern). Particle size and shape parameters are defined on Malvern Panalytical's website (Malvern, 2018).

2.2.4.1 Circularity

Circularity is the ratio of the circumference of a circle (with the area equal to that of the object's projected area) to the perimeter of the object; values range from 0 to 1.

$$\text{Circularity} = \frac{2 \times \sqrt{\pi \times \text{Area}}}{\text{Perimeter}} \quad (2)$$

2.2.4.2 Convexity

Convexity is a measurement of the surface roughness of a particle, that is, how much a particle curves in or bulges. Convexity is calculated by dividing the convex hull perimeter by the actual particle perimeter. A smooth shape like a circle has a convexity of 1, while a very 'spiky' or irregular object has a convexity closer to 0.

$$\text{Convexity} = \frac{\text{Convex Hull Perimeter}}{\text{Actual perimeter}} \quad (3)$$

Where the convex hull perimeter is calculated from an imaginary elastic band that is stretched around the outline of the particle image.

2.2.4.3 Solidity

Solidity is the object's area divided by the area enclosed within the convex hull (border created by an imaginary rubber band wrapped around the object).

$$\text{Solidity} = \frac{\text{Area}}{\text{Convex Hull Area}} \quad (4)$$

2.2.4.4 Aspect ratio

The overall form of a particle can be characterized by the aspect ratio. A particle aspect ratio is obtained by dividing its width by its length. Aspect ratio values range from 0 to 1.

$$\text{Aspect ratio} = \frac{\text{Width}}{\text{Length}} \quad (5)$$

2.2.4.5 Elongation

Elongation helps identify needle-shaped particles in a sample. Elongation values range from 0 to 1.

$$\text{Elongation} = 1 - \text{Aspect ratio} = 1 - \frac{\text{Width}}{\text{Length}} \quad (6)$$

2.3 Moisture and application rates effects on wheat physical properties

2.3.1 Sampling

Bags of hard red winter wheat (HRW) were purchased from Heartland Mills (Marienthal, KS, USA) and kept in a freezer at -13°C for 72 hrs to kill any live insects. The initial grain moisture content determined using a portable moisture tester for Grain (Shore Model 930, Shore Sales Co., Rantoul, IL, USA) was about 11.8% (d.b). Grain was sifted through an aluminium sieve (Seedburo Equipment Company, Des Plaines, IL, USA) with a nominal aperture of 0.21 mm to remove dockage, shrunken, and broken kernels. Grain was further cleaned to remove foreign material and damaged kernels. Wheat samples were obtained by emptying bags of HRW in a Boerner Divider (Seedburo Equipment Company, Des Plaines, IL, USA). The Boerner Divider meets USDA-FGIS (GIPSA) specifications for official

inspections. Briefly, the sample is placed in the hopper and released by moving a slide gate located in the hopper throat, thus allowing an even dispersion over a 38 pockets-cone. The grain, after the initial separation, is rejoined into two chutes which empty out of the bottom hopper. The principle is that the sample is poured into the divider and repeatedly halved until a sample of the desired size is obtained. A total of 81 measurement samples were obtained and 27 samples were systematically selected and randomly assigned, in triplicates, to each of nine combinations of moisture and application rates. Treatments were formed by the combinations of three moisture levels (2.01±0.05%, 6.03±0.02%, and 10.02±0.01% w.b) and three mixing ratios (0.5 g/kg, 1.0 g/kg, and 2.0 g/kg). Controls consisted of clean, sound, and dust-free HRW kernels. Wheat samples (100 g; 11.8±0.2% w.b) were allowed to equilibrate to 10.0±0.01% moisture content (w.b) in a controlled humidity chamber (Table 1) based on wheat desorption isotherm at 25°C.

2.3.2 Static angle of repose

The angle of repose (AoR) is related to particle size, shape, density, surface area, and coefficient of friction (Geldart *et al*., 2006; Al-Hashemi and Al-Amoudi, 2018). The static angle of repose was determined using the conventional method described elsewhere in the literature (Kurkuri *et al*., 2012). Briefly, samples of wheat (350 g) mixed with the synthetic zeolite were poured onto an elevated plastic horizontal surface of 9cm -diameter through a funnel from a height of 6 cm. The following formula was used to determine the angle of repose:

$$\text{Angle of Repose} = (2h/D) \quad (7)$$

Where h is the height of the conical pile formed by the zeolite powder, and D is the diameter of the base of the horizontal surface (diameter of the conical pile).

2.3.3 Test weight

A Winchester cup apparatus (Seedburo Equipment Co., Des Plaines, IL, USA) was used to estimate the bulk density. Samples were made to fall from a hopper into a cup from a height of 10 cm. The cup was filled until the excess of it began to overflow. The excess sample was removed by making three zig-zag motions with a scrapper. The cup had a volume of 473.18 mL. The bulk density was calculated from the weight and volume of the sample.

$$\text{Bulk density} = \frac{\text{Weight (kg)}}{\text{Volume (m}^3\text{)}} \quad (8)$$

2.3.4 Tapped density

A cylinder of known volume (250 mL) was filled with each sample (100 g) and the cylinder was tapped 750 times (260 taps/min) using the Autotap Density Analyzer (Quantachrome Instruments, FL, USA). The tapped density was calculated from the tapped volume and weight of the samples.

$$\text{Tapped density} = \frac{\text{Weight (kg)}}{\text{Volume after tapping (m}^3\text{)}} \quad (9)$$

2.3.5 Carr Index (CI) and Hausner Ratio (HR)

Carr Index (CI) and Hausner Ratio (HR) were obtained from bulk and tapped densities measurements and were determined as follows:

$$CI = 100 \times \frac{(\text{Tapped density} - \text{Bulk density})}{(\text{tapped density})} \quad (10)$$

$$\text{HR} = \frac{\text{Tapped Density}}{\text{Bulk density}} \times 100 \quad (11)$$

2.3.6 Single kernel characterization system

The single-kernel characterization system (SKCS) (SKCS 4100, Perten instruments, Springfields, Ill.) was used to measure wheat kernel weight, moisture content, diameter, and hardness at a rate of two kernels per second and the results were reported as the average and standard deviation of these parameters from a 300-kernel sample. The working principle of the SKCS is detailed elsewhere in the literature (Martin *et al*., 1991).

2.4 Statistical analysis

Two independent studies following a completely randomized experimental design (CRD) were subjected to:

1) One-way analysis of variance (ANOVA) was used in SAS PROC GLM procedure (SAS, 2009) to assess the significance of "dust moisture" main effect in particle size, and particle shape tests. Treatments means were separated by Bonferroni multiple comparisons test (α = 0.05)

2) Two-way ANOVA was used to assess the significance of "dust moisture" the main effect, "application rate" main effect, and their interaction (dust moisture x application rate) in physical tests related to wheat mixed with the amorphous dust. Treatments (the control was excluded) means were separated by Ryan-Einot-Gabriel-Welsch (REGW) multiple comparisons test (α = 0.05). Dunnett's multiple comparison procedure was used to compare the least-squares means of all treatments to the control (α = 0.05).

3. Results and discussion

3.1 Physical characterization of a synthetic amorphous zeolite

3.1.1 X-ray diffraction

The amorphous nature of the zeolite powder was

confirmed by the absence of a peak in the x-ray diffraction profile (Figure 1). Typical graphs for crystalline materials exhibit several peaks corresponding to specific minerals. The amorphous nature of the synthetic zeolite is required if it was intended as a grain protectant. Strict regulations exist that prohibit the application of crystalline powder onto grain intended for human consumption (Subramanyam and Roesli, 2000; Fruijtier-Pölloth, 2016).

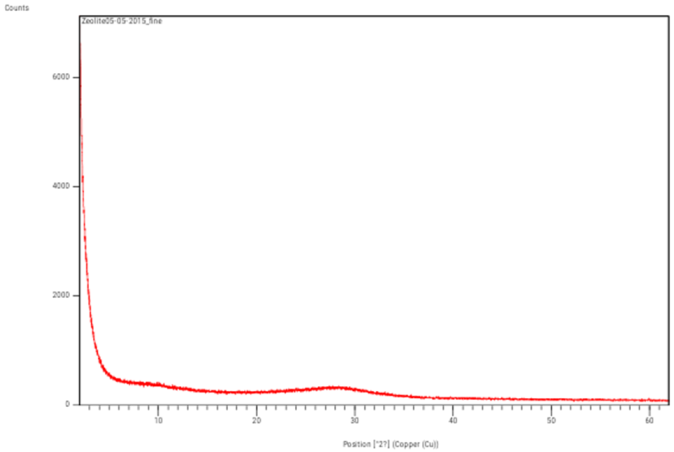

Figure 1. X-ray diffraction profile of Odor-Z-Way, a synthetic amorphous zeolite

3.1.2 Scanning electron microscopy

Scanning electron microscopy (SEM) images qualitatively show that the zeolite particles have rough edges (Figure 2). This roughness could impact the bulk flow characteristics of grain and could cause high wear on grain handling equipment. The surface texture was further investigated through image analysis.

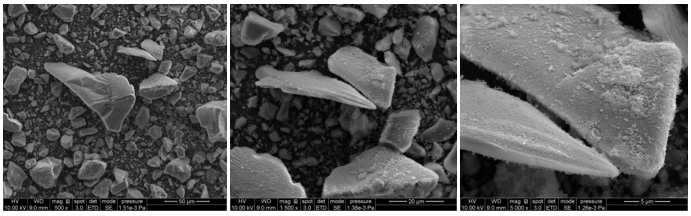

(a) (b) (c)

Figure 2. SEM micrographs of a synthetic amorphous zeolite at 500× (a), 1500× (b), and 5000× (c).

3.1.3 Specific surface area and pore characteristics of a synthetic zeolite

The characterization of specific surface area, pore volume and pore size is important to understand the moisture-solid interactional behaviour exhibited by synthetic zeolite powders. Specific surface area, pore-volume, and pore diameter were respectively: 0.556 m^2/g, 0.52 cm^3/g, and 9.14 nm. A larger specific surface area is desired because it is often correlated with the higher efficacy of the dust used as a grain protectant. The pore diameter of the zeolite particles is comprised between 2-50 nm, which is mostly the characteristic of mesoporous solids and is indicative of a Type IV sorption profile with multilayer adsorption followed by capillary condensation (Kruk and Jaroniec, 2001).

3.1.4 Particle size and size distribution

The size of the majority of the synthetic zeolite particles was below 71.84 µm. The span of the distribution indicated that the synthetic amorphous zeolite had a narrow distribution (Table 2). The narrow distribution of particles is preferred because the particles will then have uniform density characteristics.

Table 2. Physical characterization of a synthetic amorphous zeolite

Parameter	Mean±SD
BET Specific surface area (m^2/g)	0.556±0.02
Sauter Mean (µm)	18.6±1.9
De Brouckere Mean (µm)	46.8±2.4
Dv10	18.84±0.08
Dv50	37.38±0.05
Dv90	71.84±0.13
Span	1.47
Aspect ratio	0.80±0.122
Circularity	0.923±0.071
Convexity	0.958±0.047
Solidity	0.975±0.026
BJH Pore volume (cm^3/g)	0.52±0.02
BJH pore diameter (nm)	9.14±0.02
Bulk density (kg/m^3)	342.5±0.81
Tapped density (kg/m^3)	680.5±0.49
True density (g/cm^3)	2.72±0.01
Hausner ratio	1.987±0.03
Carr Index	0.497±0.05
Angle of repose (°)	47.2±6.4

3.1.5 Particle shape of a synthetic zeolite

The shape characteristics are listed in Table 2. The average circularity, convexity, and solidity of zeolite indicate that the powders are more regular shaped and closer to resembling a uniform shaped particle. However, a low aspect ratio indicates the existence of irregular shaped particles or powders with high surface irregularity (Figure 2). This surface irregularity and irregular shape of particles could influence the handling characteristics of grain treated with the amorphous zeolite.

3.1.6 Density and flow properties

Three density indicators (bulk, tapped, and true densities) were determined at the time of reception of the zeolite powder. The moisture content at the time of reception was about 35% and density indicators were respectively 342.5 kg/m^3, 680.5 kg/m^3, and 2.72 g/cm^3

for bulk density, tapped density, and true density. The corresponding values of the Hausner ratio (HR) and Carr Index (CI) were respectively 1.987±0.03 and 0.497±0.05. The angle of repose measured at the time of reception was about 47.2±6.4°. High variability observed in values of angle of repose can be explained by the manner grain was handled before and during the formation of conical piles. A comparison of HR, CI, and AOR values to the reference values indicate that the silica dust is more likely to exhibit poor flowability.

3.2 Moisture effects on amorphous dust physical properties

3.2.1 Moisture effect on particle size

Within the 2-35% moisture range, surface mean diameter significantly decreased (F = 331; P<0.0001) with increasing moisture content. Conversely, the volume mean significantly increased (F = 3807; P<0.0001) with increasing dust moisture content (Table 3). The surface mean or Sauter diameter is relevant to a specific surface area. Silica dust with a high relative frequency of fines will have a larger specific area, which is directly related to its surface coverage. Theoretically, amorphous dust with larger specific surface areas should perform better as grain protectants because of better coverage of insect cuticles with the silica dust (Korunic, 1998; Fields *et al.*, 2001; Athanassiou *et al.,* 2005; Subramanyam and Hagstrum, 2012; Eroglu *et al.,* 2017). Decreases in surface mean diameter values with increasing moisture content suggest the formation of agglomerates. Volume moment mean or De Brouckere mean diameter is indicative of the particle size which constitutes most of the bulk of the sample volume. Increases in volume mean diameter with increasing moisture show that the proportion of large particulates is increasing in the particle size distribution. The particle size distribution of the zeolite powder, reported as percentiles, is presented in Table 4. The Dv10, Dv50, and Dv90 represent the particle diameter below which 10%, 50%, and 90% respectively of the sample volume exists. In general, the one-way ANOVA indicated that all three percentiles determined at 35% moisture content were significantly higher than the percentiles determined at 2.0, 6.0, and 10.0% moisture content, which implies a significant increase in the particle size when dust moisture reaches 35%. No significant difference was found between median particle sizes (Dv50) at 2% and 6% dust moisture content, but the median particle size at 10% was significantly higher than the median particle sizes at 2% and 6%. Our data suggest that significant changes in the median particle size begin to occur at 10% dust moisture content and the maximum change in particle size occur when the dust is at 35% moisture content, that is, at the time of reception. Also, changes at the extremes of the particle size distribution (Dv10% and Dv90%) could be due to the presence of fewer fines, more oversized particles or agglomerates, or a loss in texture and structure occurring above the critical water activity.

Table 3. Surface and volume mean diameters of zeolite powder at various moisture contents.

Moisture content (%)	Mean particle size (µm)	
	Surface mean diameter ($D_{3,2}$)	Volume mean diameter ($D_{4,3}$)
2	21.3±1.2[a]	33.3±1.5[d]
6	20.8±2.7[b]	32.6±4.1[c]
10	20.0±0.9[c]	37.8±0.5[b]
35.0*	18.6±1.9[d]	46.8±2.4[a]

*Moisture content at reception, before drying cycles

Table 4. Particle size distribution of zeolite powder at various moisture contents.

Moisture content (%)	Size distribution		
	Dv10 (µm)	Dv50 (µm)	Dv90 (µm)
2	11.36[c]	31.7[b]	57.33[d]
6	11.0[d]	30.6[c]	59.08[c]
10	12.9[b]	32.7[b]	63.88[b]
35.0*	18.84[a]	37.38[a]	71.84[a]

*Moisture content at reception, before drying cycles

3.2.2 Moisture effect on particle shape

Circularity quantifies the deviation of a particle shape from a perfect circle. A perfect circle has a Circularity of 1.0, while a very narrow elongated object has a circularity close to 0. Circularity values were comprised between 0.923 and 0.979 when the moisture of the dust ranged between 2 and 35%. Particles of the amorphous dust were not close to resembling a perfect circle (Table 5). A significant decrease in circularity values was observed at 10 and 35% moisture contents. No significant difference was observed between circularity at 2 and 6% moisture contents (P<0.001). Deviation from a perfect circle was significantly higher at 35% moisture content. These changes in circularity suggest possible changes in particle form and/or outline (surface roughness).

Table 5. Median particle shape parameters of zeolite powder at various moisture contents

Moisture content (%)	Shape parameters			
	Aspect ratio	Circularity	Convexity	Solidity
2	0.74[c]	0.979[b]	0.977[b]	0.978[b]
6	0.75[c]	0.934[c]	0.978[b]	0.994[a]
10	0.77[b]	0.983[a]	0.996[a]	0.995[a]
35.0*	0.80[a]	0.923[d]	0.958[d]	0.975[b]

*Moisture content at reception, before drying cycles

Aspect ratio ranged between 0.74 and 0.79 within the 2-35% moisture range, implying that the amorphous dust particles do not have regular symmetry, such as spheres or cubes and their shape is closer to ovoid

particles, which is corroborated by the scanning electron microscopy images obtained at magnification 500×, 1500× and 5000× (Figure 2). Solidity and convexity data provided more precise information about the outline of the particles. At 2% moisture content, convexity and solidity were respectively 0.977 and 0.978, whereas, at 35% moisture content, these values dropped at 0.958 and 0.975, respectively. As with circularity, the values determined for aspect ratio, convexity, and solidity did not significantly change at 2% and 6% moisture contents. Aspect ratio, convexity, and solidity values were significantly lower at 35% moisture content, followed by 10% moisture content. These lower convexity/solidity values show that the amorphous dust particles possess rough outlines and they become agglomerated primary particles as moisture increases.

3.3 Moisture and application rates effects on wheat physical properties

3.3.1 Static angle of repose

Values of the static angle of repose can serve as an indirect assessment of flowability because the angle of repose relates to the inter-particulate friction. Changes in the bulk density of wheat were dependent on both the dust moisture and the rate of the application. In fact, the moisture main effect (F = 2489; P<0.0001) and the rate main effect (F = 117; P<0.0001) were significant at the 5% level of significance. The moisture by rate interaction was also significant at a 5% level (F = 5.0; P = 0.0018). The lowest increase in the static angle of repose was observed when wheat was admixed with the zeolite powder at 2% moisture content and an application rate of 0.5 g/kg. The highest increase in the static angle of repose was observed when wheat was mixed with the zeolite powder at 35% moisture content and an application rate of 2.0 g/kg, highlighting the importance of drying down the amorphous dust before application. Carr (1965) has proposed a classification of flowability based on the angle of repose: angles of repose below 30^o indicate good flowability, 30^o-45^o some cohesiveness, 45^o-55^o true cohesiveness, and >55^o sluggish or very high cohesiveness and very limited flowability. Based on this classification, wheat treated with the zeolite powder evolved from having “some cohesiveness” into exhibiting “true cohesiveness”.

3.3.2 Bulk and tapped density

Tests on bulk density showed that the moisture main effect (F = 8248.51; P<0.0001), the rate main effect (F = 662.69; P<0.0001), and the moisture by rate interaction (F = 57.11; P<0.0001) were all significant at the 5% level of significance. Similarly, tests on tapped density indicated that the moisture main effect (F = 50547.8; P<0.0001), the rate main effect (F = 3362.64; P<0.0001, and the moisture by rate interaction (F = 631.39; P<0.0001) were all significant at the 5% level of significance. An increase in both the dust moisture and the rate of application significantly decreased wheat bulk density and significantly increased wheat tapped density. Only minimal changes in bulk density (decrease) and in tapped density (increase) occurred when wheat was mixed with 0.5 g/kg dust at 2% moisture content. As with the static angle of repose, the highest increase in tapped density of wheat and the highest decrease in the bulk density of wheat were observed when wheat was mixed with 2.0 g/kg of zeolite powder at 35% moisture content. As a result, the combination of the highest dosage rate and the highest moisture content of the amorphous dust maximize the cohesiveness level and does not guarantee dust maximal efficacy.

3.3.3 Carr Index (CI) and Hausner Ratio (HR)

There was a significant moisture main effect (F = 8248.51; P<0.0001), a significant rate main effect (F = 662.69; P<0.0001), and a significant interaction between moisture and rate (F = 57.11; P<0.0001) at 5% level of significance. In general, higher values of CI or HR were observed for combinations of higher dust moisture contents and higher rates of application. Carr Index (CI) and Hausner Ratio (HR) are single index parameters often used to indirectly assess the flowability of a given powder or granular material. An increase in both the CI and the HR is indicative of a cohesive material with a tendency to not flow easily or a tendency to resist flow.

3.3.4 Single Kernel Characterization System (SKCS)

The data for the SKCS of wheat treated with dust at various moisture and rates is featured in Table 6. The SKCS model 4100 classifies wheat grain samples into classes of hard, soft, or mixed wheat. Hardness values were close to 75 which are typical of hard wheat, whereas hardness values close to 25 would be indicative of soft wheat. The two-way analysis of variance did not show any significant difference in wheat kernel diameter (F = 1.47; P = 0.206), and in wheat hardness (F = 0.37; P = 0.95). However, data on wheat weight and moisture content showed a significant interaction between dust moisture and rate of application (P<0.05). Wheat moisture and wheat weight were significantly higher when dust moisture was 35%. The moist dust tends to better adhere to wheat kernels, causing an apparent increase in kernel weight and moisture. Several studies have correlated a decrease in kernel hardness with an increase in kernel moisture content as described by Gaines *et al*. (1996). Our data suggest that the treatment of wheat kernels with amorphous dust at 35% moisture content increases kernel moisture which in turn decreases kernel hardness. Such a high level of dust

moisture is typically encountered at the time of reception of dust samples, following transportation and/or storage under various environmental conditions. It is essential to verify the moisture of any sample of amorphous dust intended for grain protection and make necessary adjustments before grain treatment.

4. Conclusion

The particle size of the amorphous dust increased with increasing dust moisture content. Shape parameters decreased with increasing dust moisture contents. While the bulk density of treated wheat kernels decreased, the tapped density and the angle of repose rather increased, resulting in higher Hausner ratios and Carr Index values. Treating wheat with the amorphous dust at the highest moisture (35%) and application rate (2.0 g/kg) caused the treated wheat to transition from an acceptable flowability to a poor flowability along with a decrease in wheat kernel hardness. A range of moisture content (2-6%) and an application rate (0.5 g/kg) mitigated the adverse effects on wheat flowability. The improper handling of the amorphous dust before analysis may induce significant biases in the analysis of the flow and the physical properties of amorphous silica dust and ultimately that of inert dust treated wheat kernels.

Conflicts of interest

The authors declare no conflict of interest.

Acknowledgements

This paper is contribution no. 21-312-J from the Kansas Agricultural Experiment Station. We would like to thank the Government of Australia (Department of Industry and Science, Plant Biosecurity Cooperative Research Center, Grant No. 63058). We think particularly of Dr Michael Robinson, CEO and currently Managing Director of the Australian Plant Biosecurity Science Foundation (APBSF). We express our heartfelt gratitude to Dr. David Eagling (Research Coordinator and Safeguarding Trade Program Leader), Dr. Jo Luck (Director Research, Education and Training), and Ern Kostas (Internship supervisor). We extend our gratitude to grain protection coordinators across Western Australia for their technical support: Guy Baxter (Kwinana Terminal), Shaugn Tomlinson (Metro Grain Centre), Mario Discenza and Casey Atkinson (Merredin), Keith Andrew and Trevor Martins (Albany Terminal).

References

Al-Hashemi, H.M.B. and Al-Amoudi, O.S.B. (2018). A review on the angle of repose of granular materials. *Powder Technology*, 330(8), 397-417. https://doi.org/10.1016/j.powtec.2018.02.003

Altuntaş, E. and Yıldız, M. (2007). Effect of moisture content on some physical and mechanical properties of faba bean (*Vicia faba* L.) grains. *Journal of Food Engineering*, 78(1), 174-183. https://doi.org/10.1016/j.jfoodeng.2005.09.013

Andrews, S., Nover, D. and Schladow, S.G. (2010). Using laser diffraction data to obtain accurate particle size distributions: the role of particle composition. *Limnology and Oceanography, Methods*, 8(10), 507-526. https://doi.org/10.4319/lom.2010.8.507

Athanassiou, C.G., Kavallieratos, N.G., Economou, L.P., Dimizas, C.B., Vayias, B.J., Tomanović, S. and Milutinović, M. (2005). Persistence and efficacy of three diatomaceous earth formulations against *Sitophilus oryzae* (Coleoptera: Curculionidae) on wheat and barley. *Journal of Economic Entomology*, 98(4), 1404-1412. https://doi.org/10.1603/0022-0493-98.4.1404

Eggers, J., Kempkes, M. and Mazzotti, M. (2008). Measurement of size and shape distributions of particles through image analysis. *Chemical Engineering Science*, 63(22), 5513-5521. https://doi.org/10.1016/j.ces.2008.08.007

Emery, E., Oliver, J., Pugsley, T., Sharma, J. and Zhou, J. (2009). Flowability of moist pharmaceutical powders. *Powder Technology*, 189(3), 409-415. https://doi.org/10.1016/j.powtec.2008.06.017

Eroglu, N., Emekci, M. and Athanassiou, C.G. (2017). Applications of natural zeolites on agriculture and food production. *Journal of the Science of Food and Agriculture*, 97(11), 3487-3499. https://doi.org/10.1002/jsfa.8312

Eshel, G., Levy, G.J., Mingelgrin, U. and Singer, M.J. (2004). Critical evaluation of the use of laser diffraction for particle-size distribution analysis. *Soil Science Society of America Journal*, 68, 736-743.

Fields, P., Korunic, Z. and Fleurat-Lessard, F. (2001). Control of insects in post-harvest: inert dusts and mechanical means. In Vincent, C., Panneton, B. and Fleurat-Lessard, F. (Eds.), Physical Control Methods in Plant Protection, p. 248-260. Berlin, Germany: Springer Science and Business Media. https://doi.org/10.1007/978-3-662-04584-8_17

Fitzpatrick, J.J., Barringer, S.A. and Iqbal, T. (2004). Flow property measurement of food powders and sensitivity of Jenike's hopper design methodology to the measured values. *Journal of Food Engineering,* 61(3), 399-405. https://doi.org/10.1016/S0260-8774(03)00147-X

Freeman, R. (2007). Measuring the flow properties of

consolidated, conditioned and aerated powders—a comparative study using a powder rheometer and a rotational shear cell. *Powder Technology*, 174(1-2), 25-33. https://doi.org/10.1016/j.powtec.2006.10.016

Freeman, R. and Cooke, J. (2006). Understanding powder behaviour by measuring bulk, flow and shear properties. *Pharmaceutical Technology Europe*, 18 (11), 39-40.

Fruijtier-Pölloth, C. (2016). The safety of nanostructured synthetic amorphous silica (SAS) as a food additive (E 551). *Archives of Toxicology*, 90(12), 2885-2916. https://doi.org/10.1007/s00204-016-1850-4

Fu, Q. and Sun, W. (2001). Mie theory for light scattering by a spherical particle in an absorbing medium. *Applied Optics,* 40(9), 1354-1361. https://doi.org/10.1364/AO.40.001354

Fu, X., Huck, D., Makein, L., Armstrong, B., Willen, U. and Freeman, T. (2012). Effect of particle shape and size on flow properties of lactose powders. *Particuology*, 10(2), 203-208. https://doi.org/10.1016/j.partic.2011.11.003

Gaines, C.S., Finney, P.F., Fleege, L.M. and Andrews, L.C. (1996). Predicting a hardness measurement using the single-kernel characterization system. *Cereal chemistry*, 73(2), 278-283.

Ganesan, V., Rosentrater, K.A. and Muthukumarappan, K. (2008). Flowability and handling characteristics of bulk solids and powders–a review with implications for DDGS. *Biosystems Engineering,* 101(4), 425-435. https://doi.org/10.1016/j.biosystemseng.2008.09.008

Geldart, D., Abdullah, E.C., Hassanpour, A., Nwoke, L.C. and Wouters, I.J.C.P. (2006). Characterization of powder flowability using measurement of angle of repose. *China Particuology*, 4(3-4), 104-107. https://doi.org/10.1016/S1672-2515(07)60247-4

Iqbal, T. and Fitzpatrick, J.J. (2006). Effect of storage conditions on the wall friction characteristics of three food powders. *Journal of Food Engineering*, *72*(3), 273-280. https://doi.org/10.1016/j.jfoodeng.2004.12.007

Korunic, Z. (1998). Review Diatomaceous earths, a group of natural insecticides. *Journal of Stored Product Research*, 34(2-3), 87-97. https://doi.org/10.1016/S0022-474X(97)00039-8

Kruk, M. and Jaroniec, M. (2001). Gas adsorption characterization of ordered organic-inorganic nanocomposite materials. *Chemistry of Materials,* 13 (10), 3169-3183. https://doi.org/10.1021/cm0101069

Kurkuri, M.D., Randall, C. and Losic, D. (2012). New method of measuring the angle of repose of hard wheat grain, presented at Chemeca: Quality of Life through Chemical Engineering. Wellington, New Zealand.

Lumay, G., Boschini, F., Traina, K., Bontempi, S., Remy, J., Cloots, R. and Vandewalle, N. (2012). Measuring the flowing properties of powders and grains. *Powder Technology*, 224(9), 19-27. https://doi.org/10.1016/j.powtec.2012.02.015

Malvern Panalytical. (2018). Particle size and shape analysis. Retrieved on June 3, 2018 from Malvern Panalytical's website: www.panalytical.com/en/learn/knowledge-center/user-manuals/MAN0410EN

Martin, C.R., Rousser, R. and Brabec, D.L. (1991). Rapid Single Kernel Grain Characterization System U.S. Patent No. 5,005,774. Washington, DC, USA: U.S. Patent and Trademark Office.

Niskanen, I., Forsberg, V., Zakrisson, D., Reza, S., Hummelgård, M., Andres, B. and Thungström, G. (2019). Determination of nanoparticle size using Rayleigh approximation and Mie theory. *Chemical Engineering Science*, 201(9), 222-229. https://doi.org/10.1016/j.ces.2019.02.020

Subramanyam, B. and Hagstrum, D.W. (2012). Alternatives to pesticides in stored-product IPM. Boston, USA: Springer Science and Business Media.

Subramanyam, B. and Roesli, R. (2000). Inert dusts. In Subramanyam, B. and Hagstrum, D. (Eds.), Alternatives to pesticides in stored-product IPM, p. 321-380. Boston, USA: Springer Science and Business Media. https://doi.org/10.1007/978-1-4615-4353-4_12

